

# **Lg WAVE PROPAGATION USING SH AND P AND SV SCREEN PROPAGATORS IN HETEROGENEOUS CRUSTS WITH IRREGULAR TOPOGRAPHY**

Ru-Shan Wu, Xiao-Bi Xie and Xian-Yun Wu  
Institute of Tectonics, University of California, Santa Cruz

Sponsored by U.S. Department of Defense  
Defense Threat Reduction Agency

Contract No. DSWAO 1 -97-1-0004

## **ABSTRACT**

This study is aimed at development and application of new wave propagation and modeling methods for regional waves in heterogeneous crustal waveguides using one-way wave approximation. The half-space generalized screen propagators (GSP) for both SH and P-SV waves have taken the free surface into the formulation and adopt a fast dual domain implementation. The method is several orders of magnitude faster than finite-difference method with a similar accuracy for certain problems. It has been used for the simulation of wave propagation for high-frequency waves (1-25Hz) to a regional distance (greater than 1000km).

In this year, we further develop the method in two fronts. First, we extend the SH GSP method to treat irregular surface topography by incorporating a coordinate transform into the method. It is demonstrated that our new approach has superior wide-angle response to surface topography over the PE (parabolic equation) method. The efficiency of the screen propagator approach makes it very promising for long distance Lg simulation. For a test model with a propagation distance of 250km and a dominant frequency of 1Hz, the screen method took about 35 minutes, while the boundary element method took about 72 hours. For longer propagation distances and higher frequencies, the factor of saving could be huge.

Second, we developed a P-SV screen propagator for crustal waveguides with flat surfaces. This is the major task of this year. Free surface reflection and conversion have been incorporated into the screen propagator theory. Numerical tests have been done against the wavenumber integration and finite-difference calculations. The results demonstrated the feasibility of the approach.

Finally, numerical simulations have been conducted for various crustal waveguide structures, including deterministic structures, small-scale random heterogeneities and random rough surfaces. Influences of random heterogeneities and rough surfaces on Lg amplitude attenuation and Lg coda formation have been studied.

## **INSTRUCTION**

Short-period regional phases ( $P_n$ ,  $P_g$ ,  $S_n$ ,  $L_g$ , etc.) play an important role for both discrimination and yield estimation procedures for monitoring the Comprehensive Nuclear-Test-Ban Treaty (CTBT). Amplitude ratios of short-period P wave energy ( $P_n$ ,  $P_g$ ) to S wave energy ( $S_n$ ,  $L_g$ ) have emerged as particularly promising discriminants, especially at frequencies above 3Hz (Walter et al., 1995; Taylor, 1996; Hartse et al., 1997; Fan and Lay, 1998). Regional phases mainly propagate in the crustal waveguide and the uppermost mantle. A wide variety of observational and theoretical studies show that the structure and multi-scale heterogeneities of the crustal wave guide and uppermost mantle strongly affect the regional phases in waveform properties and amplitudes (Kennett, 1986, 1989; Zhang et al., 1994; Fan and Lay, 1998). However, due to the complexity involved in regional phase propagation and limit of capability of the existing analysis and simulation approaches, the mechanism of excitation and propagation of regional phases is still not appreciated. In these investigations, numerical approaches for simulating regional phases are very useful.

In the crustal waveguide environment, major wave energy is carried by forward propagating waves, including forward scattered waves, therefore neglecting backscattered waves in the propagation will not change the main features of regional waves in most cases. Based on the concept, a generalized screen propagator method (GSP) based on one-way wave equation has been developed by Wu (1994), Wu, Jin and Xie (1999a) and has been successfully used to simulate SH Lg waves in the complex crustal waveguide and investigate the energy partitioning of Lg waves (Wu, Jin and Xie, 1999b). Wu, Xie and Wu (1999) further extended the GSP method to treat complex crustal waveguides with irregular or rough topography by incorporating a surface topographic transformation into the method. For a test model with propagation distance of 250km, dominant operating frequency of 1Hz, the BE (boundary element) method took about 72 hours, while the screen method took only 35 minutes with the same accuracy. For longer propagation distances and higher frequencies, the factor of saving could be huge.

Based on the success of Lg propagation using SH screen propagators, in this paper we extend the screen propagator method to P-SV Lg wave propagation. As the first step we apply the complex screen method to a flat, heterogeneous half space. Unlike SH wave, the image method can not be used to account for the effect of free surface. We incorporate the reflection coefficient calculations of elastic waves on free surface into the complex screen method for the effect of free surface on P-SV waves. Comparison of synthetic seismograms calculated by the complex screen method and wavenumber integration method for an elastic half-space shows feasibility and validity of the approach. Synthetic seismograms for elastic layered model and a laterally varying crustal waveguide are conducted and compared with wavenumber integration method and finite difference method, respectively. The results demonstrate that the complex screen method can be used to model regional phases containing  $P_n$ ,  $P_g$ ,  $S_n$  and  $L_g$ .

## **METHODOLOGY**

Figure 1 illustrates the principle of the method. The screen method is a forward matching algorithm. To avoid the energy increase caused by the repetitive application of reflection calculation, we extend the model in vertical direction from free surface, and the extended part has the parameters of background medium. The complex screen method will be applied to such an extended model for elastic wave simulation. For each forward step we apply the reflection calculation to the incident field (only to upgoing waves) to get the reflections and conversions from free surface. Figure 1 also shows such a process by an upgoing ray from source. Knowing the reflections and

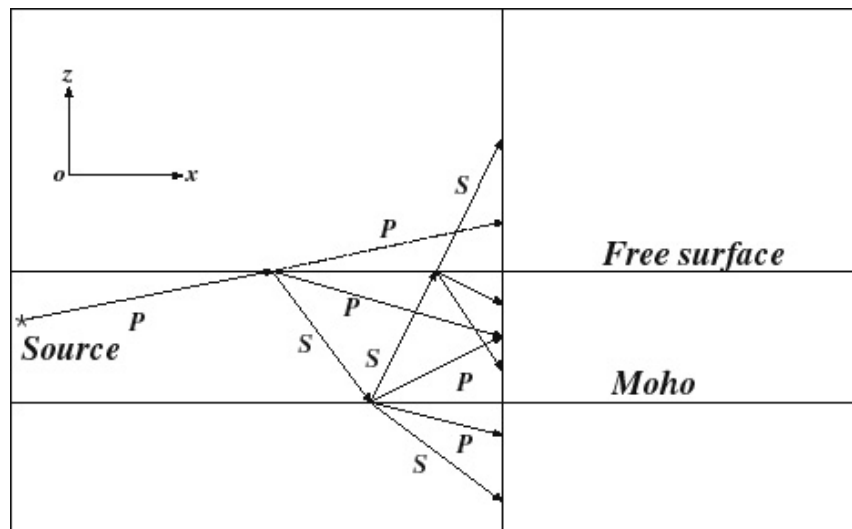


**Figure 1. Illustration of the screen method**

conversions, we can calculate the scattered field of the reflected fields using the complex screen method and then combine the scattered field into the incident field to obtain new incident field. In the following, a simple description of the complex screen method and reflection coefficient formulas will be given.

### **COMPLEX SCREEN APPROXIMATION FOR ELASTIC WAVES**

A complete derivation of the complex screen method for modeling elastic waves can be seen in Wu's papers (Wu, 1994, 1996). A short review of the method for foreshattering is given in this section. Suppose that the parameters of the elastic medium and the total wave field can be expressed as

$$\begin{aligned}\rho(\mathbf{x}) &= \rho_0 + \delta\rho(\mathbf{x}) \\ \alpha(\mathbf{x}) &= \alpha_0 + \delta\alpha(\mathbf{x}) \\ \beta(\mathbf{x}) &= \beta_0 + \delta\beta(\mathbf{x})\end{aligned}$$

and

$$u(\mathbf{x}) = u_0 + U(\mathbf{x})$$

where  $\rho_0$ ,  $\alpha_0$  and  $\beta_0$  are the parameters of the background medium,  $\delta\rho(\mathbf{x})$ ,  $\delta\alpha(\mathbf{x})$  and  $\delta\beta(\mathbf{x})$  are the corresponding perturbations,  $u_0$  and  $U(\mathbf{x})$  are the incident field and the scattered field,  $\mathbf{x} = x\mathbf{e}_x + z\mathbf{e}_z$  is a 2-D position vector in Cartesian coordinates. We take  $\mathbf{e}_x$  to be the primary propagation direction perpendicular to the thin slab. The incident field  $u_0$  at  $x_0$ , i.e., the entrance of the thin slab, can be decomposed into plane P and S waves

$$u_0(\mathbf{x}) = \frac{1}{4\pi^2} \int dk [u_0^P(k, x_0) + u_0^S(k, x_0)] e^{ikz} \quad (1)$$

where  $k$  is the transverse wavenumber of plane waves. Superscripts P and S denote P and S waves, respectively. The forward propagated field is composed of primary wave and forward scattered P and S waves. Therefore, at  $x_1$  the exit of the thin slab, it can be expressed as

$$u_f(z, x_1) = \frac{1}{4\pi^2} \int dk [u_f^P(k, x_1) + u_f^S(k, x_1)] e^{ikz} \quad (2)$$

where

$$u_f^P(z, x_1) = \left\{ e^{i\gamma_\alpha \Delta x} u_0^P(k, x_0) + u_f^{PP}(k, x_1) + u_f^{SP}(k, x_1) \right\} \quad (3)$$

$$u_f^S(z, x_1) = \left\{ e^{i\gamma_\beta \Delta x} u_0^S(k, x_0) + u_f^{SS}(k, x_1) + u_f^{PS}(k, x_1) \right\} \quad (4)$$

where  $\gamma_\alpha = (k_\alpha^2 - k^2)^{1/2}$  and  $\gamma_\beta = (k_\beta^2 - k^2)^{1/2}$  are the  $x$  components (propagating wavenumber) of P and S wavenumbers in the background medium.  $k_\alpha = \omega/\alpha$  and  $k_\beta = \omega/\beta$  are P and S wavenumbers,  $\alpha$  and  $\beta$  are P and S velocities of the background medium.  $\Delta x = x_1 - x_0$  is the thickness of thin slab. Subscripts  $f$  denotes forward scatterings, and PP, PS, SP and SS indicate the scattering between different wave types. The scattering and conversion coefficients  $U_f^{PP}$ ,  $U_f^{PS}$ ,  $U_f^{SP}$  and  $U_f^{SS}$  can be calculated by the complex screen approximation (Wu, 1994,1996).

## REFLECTIONS FOR P-SV WAVES

Suppose that a plane P (or S) wave is traveling in the background medium at a angle of  $i$  (or  $j$ ) with respect to  $x$  (see Fig. 1). The reflection coefficients of the displacement at the free surface can be written as (Aki and Richard, 1984)

$$\hat{P}^{\vee} \hat{P}^{\wedge} = \frac{-\left(\frac{1}{\beta_0^2} - 2p^2\right)^2 + 4p^2 \frac{\cos i \cos j}{\alpha_0 \beta_0}}{\left(\frac{1}{\beta_0^2} - 2p^2\right)^2 + 4p^2 \frac{\cos i \cos j}{\alpha_0 \beta_0}} \exp\left\{-2i\omega \frac{\cos i}{\alpha_0} z_{free}\right\} \quad (5)$$

$$\hat{P}^{\vee} \hat{S}^{\wedge} = \frac{4\frac{\beta_0}{\alpha_0} p \frac{\cos i}{\alpha_0} \left(\frac{1}{\beta_0^2} - 2p^2\right)}{\left(\frac{1}{\beta_0^2} - 2p^2\right)^2 + 4p^2 \frac{\cos i \cos j}{\alpha_0 \beta_0}} \exp\left\{-i\omega \left(\frac{\cos i}{\alpha_0} + \frac{\cos j}{\beta_0}\right) z_{free}\right\} \quad (6)$$

$$\hat{S}^{\vee} \hat{P}^{\wedge} = \frac{4\frac{\beta_0}{\alpha_0} p \frac{\cos j}{\beta_0} \left(\frac{1}{\beta_0^2} - 2p^2\right)}{\left(\frac{1}{\beta_0^2} - 2p^2\right)^2 + 4p^2 \frac{\cos i \cos j}{\alpha_0 \beta_0}} \exp\left\{-i\omega \left(\frac{\cos i}{\alpha_0} + \frac{\cos j}{\beta_0}\right) z_{free}\right\} \quad (7)$$

$$\hat{S}^{\vee} \hat{S}^{\wedge} = \frac{\left(\frac{1}{\beta_0^2} - 2p^2\right)^2 - 4p^2 \frac{\cos i \cos j}{\alpha_0 \beta_0}}{\left(\frac{1}{\beta_0^2} - 2p^2\right)^2 + 4p^2 \frac{\cos i \cos j}{\alpha_0 \beta_0}} \exp\left\{-2i\omega \frac{\cos j}{\beta_0} z_{free}\right\} \quad (8)$$

where  $z_{free}$  denotes the free surface location.  $p$  is ray parameter which is  $\frac{\sin i}{\alpha_0}$  for P wave incidence, and  $\frac{\sin j}{\beta_0}$  for S wave incidence. The symbol “ $\wedge$ ” and “ $\vee$ ” denote upgoing and downgoing waves, respectively. From the screen method, the incident P wave at  $x = x_0$  can be expressed as a superposition of plane waves

$$u_0^P(z, x_0) = \frac{1}{4\pi^2} \int dk u_0^P(k, x_0) e^{ikz} \quad (9)$$

Applying the reflection coefficient formulation (5-8) to the upgoing waves in eq. (9), the reflected P and S waves can be expressed by

$$u_x^{PP}(z, x_0) = \frac{1}{4\pi^2} \int dk |u_0^P(k, x_0)| \hat{P}^{\vee} \hat{P}^{\wedge} \frac{\gamma_\alpha}{k_\alpha} e^{-ikz} \quad (10)$$

$$u_z^{PP}(z, x_0) = -\frac{1}{4\pi^2} \int dk |u_0^P(k, x_0)| \hat{P}^{\vee} \hat{P}^{\wedge} \frac{k}{k_\alpha} e^{-ikz} \quad (11)$$

$$u_x^{PS}(z, x_0) = \frac{1}{4\pi^2} \int dk |u_0^P(k, x_0)| \hat{P}^{\vee} \hat{S}^{\wedge} \frac{k^{PS}}{k_\beta} e^{-ik^{PS}z} \quad (12)$$

$$u_z^{PS}(z, x_0) = \frac{1}{4\pi^2} \int dk |u_0^P(k, x_0)| \hat{P}^{\vee} \hat{S}^{\wedge} \frac{\gamma_\beta}{k_\beta} e^{-ik^{PS}z} \quad (13)$$

where  $k^{PS}$  is transverse wavenumber of the converted S wave, using Snell's law,  $k^{PS} = \sqrt{k_\beta^2 - k_\alpha^2 + k^2}$ .  $|u_0^P(k, x_0)|$  is the amplitude of incident P wave with transverse wavenumber  $k$ . In the same way, the reflected P and S waves due to the incident plane S wave can be obtained by

$$u_x^{SP}(z, x_0) = \frac{1}{4\pi^2} \int dk |u_0^S(k, x_0)| \hat{S}^{\vee} \frac{\gamma_\alpha}{k_\alpha} e^{-ik^{SP}z} \quad (14)$$

$$u_z^{SP}(z, x_0) = -\frac{1}{4\pi^2} \int dk |u_0^S(k, x_0)| \hat{S}^{\vee} \frac{k^{SP}}{k_\alpha} e^{-ik^{SP}z} \quad (15)$$

$$u_x^{SS}(z, x_0) = \frac{1}{4\pi^2} \int dk |u_0^S(k, x_0)| \hat{S}^{\vee} \frac{k}{k_\beta} e^{-ikz} \quad (16)$$

$$u_z^{SS}(z, x_0) = \frac{1}{4\pi^2} \int dk |u_0^S(k, x_0)| \hat{S}^{\vee} \frac{\gamma_\beta}{k_\beta} e^{-ikz} \quad (17)$$

where  $k^{SP}$  is the transverse wavenumber of the converted  $P$  wave,  $k^{SP} = \sqrt{k_\alpha^2 - k_\beta^2 + k^2}$ .  $|u_0^S(k, x_0)|$  is the amplitude of incident S wave with transverse wavenumber  $k$ . We can calculate all of the reflected waves using eqs. (10-17), once the incident fields  $u_0^P$  and  $u_0^S$  are known. It is not difficult to see that eqs (10-11, 16-17), i.e., the reflected waves of the same type waves, can be implemented by FFT. However, eqs (12-15), i.e., the reflected converted can not be directly implemented by FFT because the nonlinear relationship exists between  $k$  and  $k^{PS}$  for P-S (or  $k^{SP}$  for S-P). Although we can obtain uniform samples with respect to  $k$  and  $k^{PS}$  (or  $k^{SP}$ ) by complex variable interpolation, the noise due to the interpolation is so strong that the accumulated errors increase fast for multiple step propagation. In this study, the direct calculations of the summation integrals are performed for the converted reflections. The implementation of eqs (12-15) by summation is not much slower than by FFT because only limited summation is required where the conversion coefficients are not zero.

## **NUMERICAL EXAMPLES**

To test the accuracy and ability of the complex screen method used as a propagator for crustal wave guides with flat surfaces, several numerical examples have been conducted and compared with those calculated by wavenumber integration method and finite difference method. For the screen method, the spatial intervals in  $x$  and  $z$  directions are  $\Delta x = \Delta z = 0.25km$ . To reduce the effects of boundary reflection and large-angle waves, two smooth window functions are applied in space domain and wavenumber domain, respectively. The vertical components of displacement in all figures shown in this paper are multiplied by 2.

Figure 2 shows synthetic seismograms calculated by the screen method (solid) and wavenumber integration method (dashed) for an elastic half-space. (a) is the vertical component of the displacement and (b) is the horizontal component. The homogeneous elastic half-space has  $\alpha = 4km/s$ ,  $\beta = 2.5km/s$  and  $\rho = 2.5g/cm^3$ . An explosive source is located at 16km depth and has dominant frequency of 1Hz. The size of the extended model used is  $1024 \times 528$ . The first 4 receivers are placed along free surface and have the offset of 100–124km, and the last 5 receivers are placed in vertical direction and have the vertical depth 0–32km. From Figure 2 the reflection and conversion by free surface are in excellent agreement. It is also shown that the use of direct summation over incident waves for converted waves (P-S or S-P) avoids the strong noise caused due to the complex variable interpolation in wavenumber domain.

Figure 3 shows synthetic seismograms along a vertical profile at the distance of 80km calculated by the screen method (solid) and wavenumber integration method (dashed) for a 2-layered half-space model (56km). The parameters for two elastic layers are  $\alpha_1 = 6.8km/s$ ,  $\beta_1 = 3.5km/s$ ,  $\rho_1 = 3.5g/cm^3$ ,

$\alpha_2 = 8.16 \text{ km/s}$ ,  $\beta_2 = 4.2 \text{ km/s}$  and  $\rho_2 = 3.5 \text{ g/cm}^3$ . An explosive source is 28km depth and has a dominant frequency of 0.5Hz. The size of the extended model is 1024×320. From figure 3 the results from the two methods are in excellent agreement up to wide-angle reflections. The reflections from free surface are angle-dependent and agree exactly with those calculated by wavenumber integration method. The multiple reflections of S waves behind travel time of 40sec. from interface have near 90° incident angle to screens and can not be modeled accurately by the screen method. However, the multiples can not survive in the wave guide and do not contribute much to Lg waves.

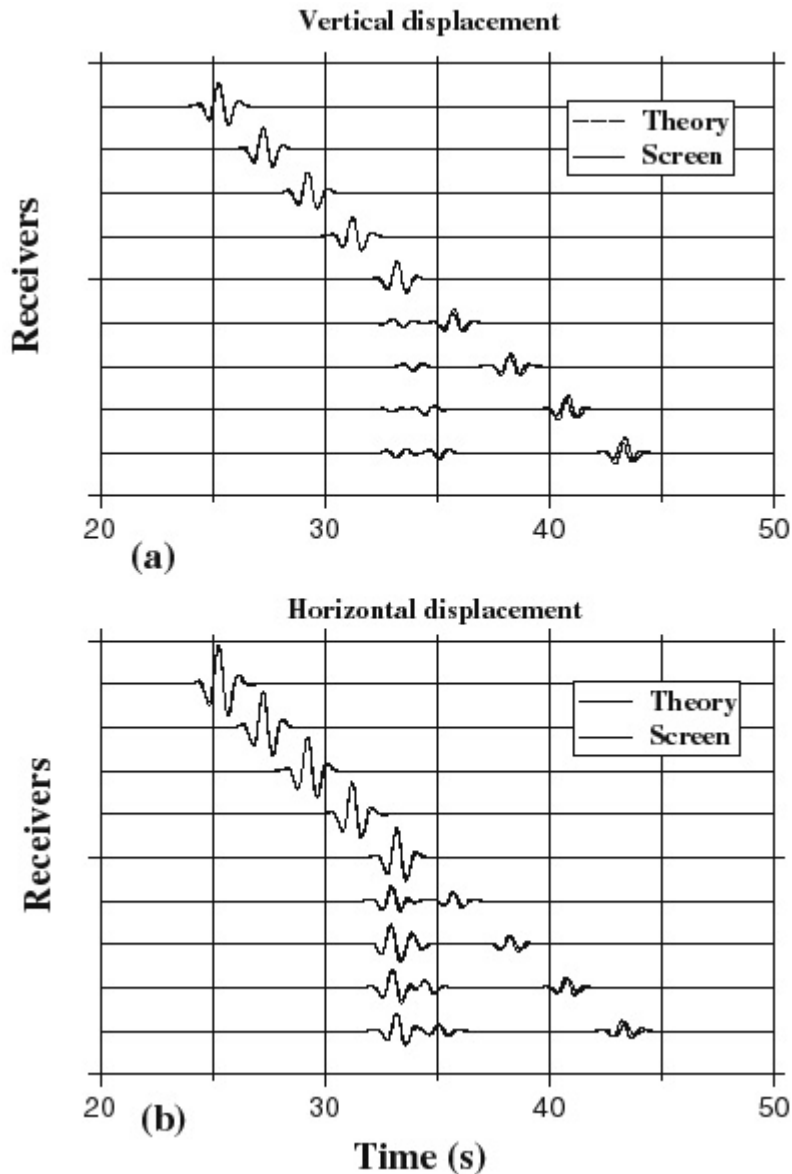
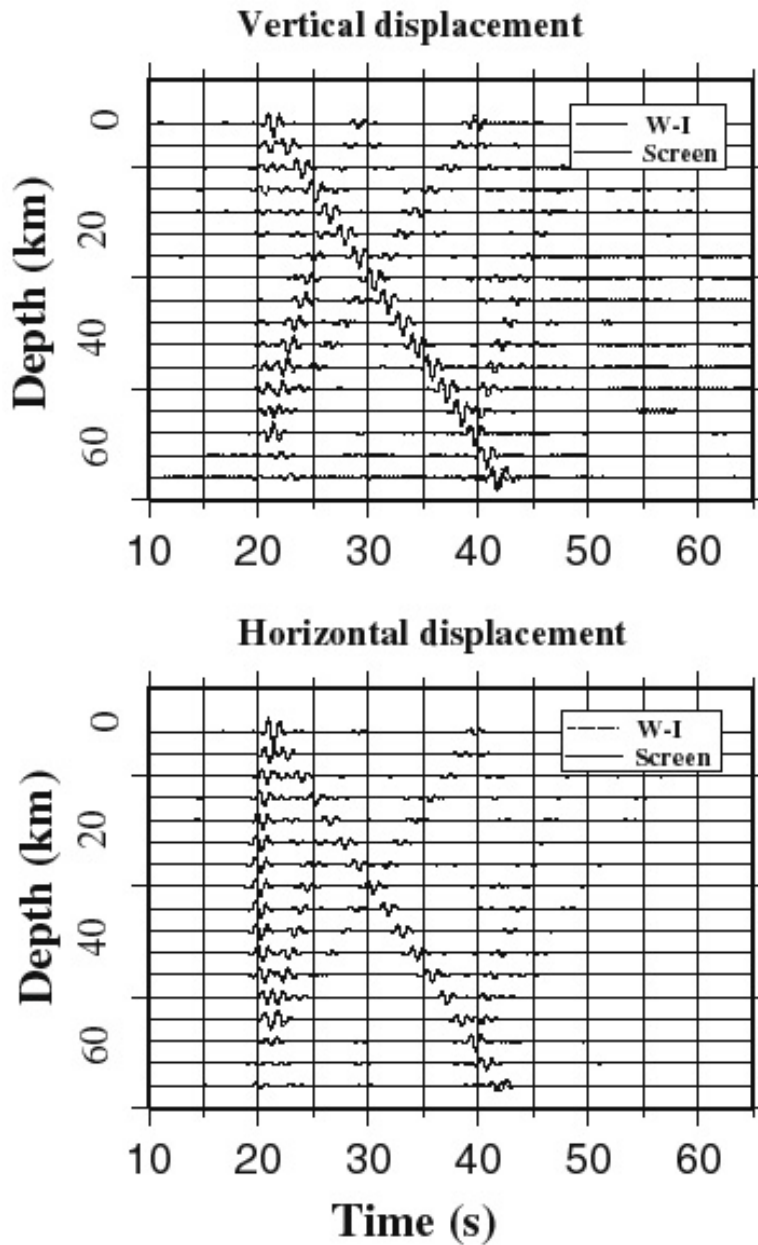


Figure 2. Synthetic seismograms calculated by the screen method (solid) and wavenumber integration (dashed) for an elastic half-space. (a) is the vertical component of the displacement, (b) is the horizontal component. An explosive source is located at 16km depth and has a dominant frequency of 1Hz. The first 4 receivers are placed along free surface, and the last 5 receivers are placed in vertical direction.



**FIGURE 3.** Synthetic seismograms along a vertical profile at the distance of  $80\text{km}$  calculated by the screen method (solid) and wavenumber integration method (dashed) for a 2 layered model ( $56\text{km}$ ). The source depth is  $28\text{km}$  and its dominant frequency is  $0.5\text{Hz}$ .

Figure 4 shows a laterally varying crustal model. The geometry of the model and the parameters are also given in Figure 4. The source is located at  $16\text{km}$  depth and has a dominant frequency of  $1\text{Hz}$ . The comparison of synthetic seismograms along vertical profile at the distance of  $200\text{km}$  calculated by the complex screen method (solid) and finite difference method (dashed) is shown in Figure 5. Excellent

agreement can be seen. While finite difference method took 51 hours on a single processor of SUN Workstation, the complex screen method took only 0.6 hour.

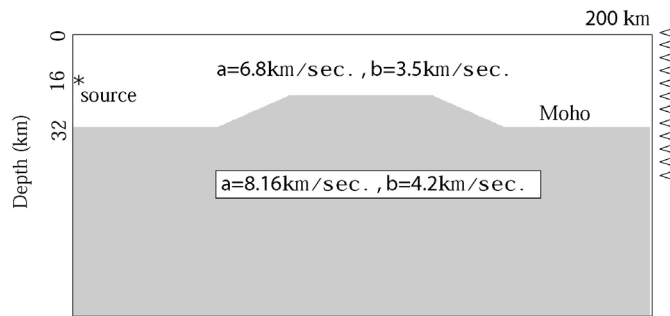


Figure 4. A thinning crustal model

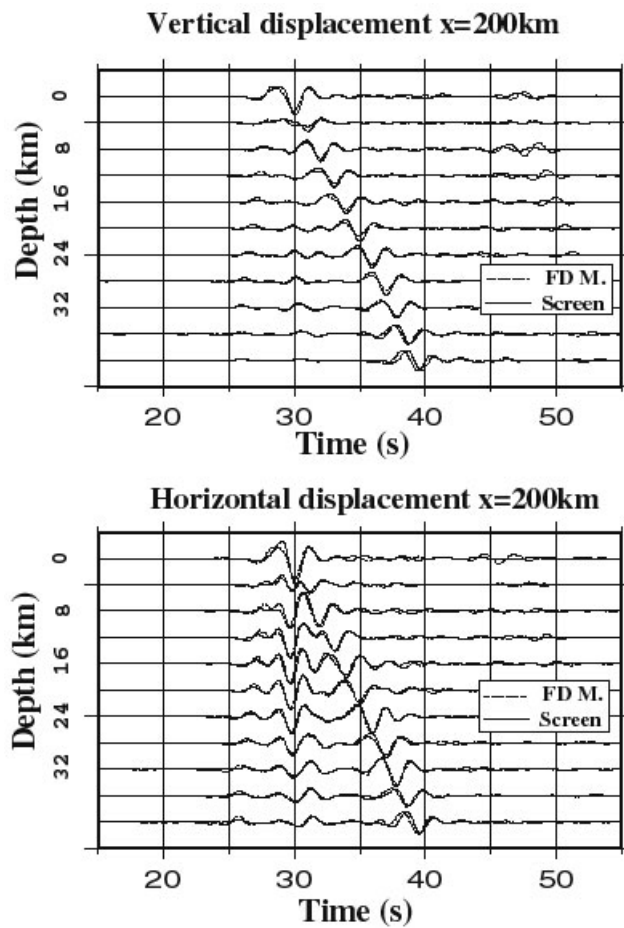


Figure 5. Synthetic seismograms along a vertical profile at the distance of 200km calculated by the screen method (solid) and finite difference method (dashed) for a thinning crustal model (32km). The source depth is 16km and its dominant frequency is 0.5Hz .

## **CONCLUSIONS**

This paper is part of the study aimed at development and application of a new wave propagation and modeling method for regional waves in heterogeneous crustal wave guides using one-way wave approximation. In this paper we extend the complex screen method to 2D P-SV problems for regional phase simulation by incorporating the reflection coefficient formulas on free surface into the method. The comparison of synthetic seismograms calculated by the complex screen method and by wavenumber integration method and finite difference method shows feasibility and validity of this extension. For a test model with a propagation distance of  $80\text{km}$  and a dominant frequency of  $0.5\text{Hz}$ , finite difference method took 51 hours, while the complex screen method took 0.6 hour. The complex screen method is 85 times faster than finite difference method. For longer propagation distance and higher frequencies, the factor of saving could be huge. By this extension, our ability of simulating regional phases will be greatly enhanced. It makes us possible to simulate path effects in different regions for various discriminants in the monitoring system, such as  $P_n / L_g$ ,  $S_n / L_g$ , etc.

**Key Words:** seismic wave propagation, crustal structure, discrimination

## **References**

- Aki, K. and P.G., Richards, 1980, Quantitative seismology: Theory and Methods, *Vol. 1 and 2*, W.H. Freeman, New York.
- Fan, G.W. and T. Lay, 1998, Statistical analysis of irregular wave-guide influences on regional seismic discriminants in China, *Bull. Seis. Soc. Am.*, 88, 74-88.
- Hartse, H.E., S.R., Taylor, W.S., Phillips, and G.E., Randall, 1997, A preliminary study of regional seismic discrimination in central Asia with emphasis on western China, *Bull. Seis. Soc. Am.*, 87, 551-568.
- Kennett, B.L.N., 1986,  $L_g$  waves and structural boundaries, *Bull. Seis. Soc. Am.*, 76, 1133-1141.
- Kennett, B.L.N., 1989, On the nature of regional seismic phases---I. Phase representations for  $P_n$ ,  $P_g$ ,  $S_n$ ,  $L_g$ , *Geophys. J.* 98, 447-456.
- Taylor, S.R., 1996, Analysis of high frequency  $P_n / L_g$  ratios from NTS explosions and western U.S. earthquakes, *Bull. Seis. Soc. Am.*, 86, 1042-1053.
- Walter, W.R., K.M., Mayeda, and H. Patton, 1995, Phase and spectral ratio discrimination between NTS earthquakes and explosions. Part I: Empirical observations, *Bull. Seis. Soc. Am.*, 85, 1050-1067.
- Wu, R.S., 1994, Wide-angle elastic wave one-way propagator in heterogeneous media and an elastic wave complex-screen method, *J. Geophys. Res.*, 99, 751-766.
- Wu, R.S., S. Jin, and X.B., Xie, 1998a, Seismic wave propagation and scattering in heterogeneous crustal waveguides using screen propagators: I  $SH$  waves. Submitted to *Bull. Seis. Soc. Am.*
- Wu, R.S., S. Jin, and X.B. Xie, 1998b, Energy partition and attenuation of  $L_g$  waves by numerical simulations using screen propagators, submitted to *Phys. Earth and Planet. Inter.*
- Wu, R.S., X.B., Xie, and X.Y., Wu, 1999,  $L_g$  wave simulations in heterogeneous crusts with irregular topography using half-space screen propagators, *Proc. of the 18th Annual SRS on Monitoring CTBT*

Xie, X.B. and Z.X. Yao, 1988, *P-SV* wave responses for a point-source in two-dimensional heterogeneous media: finite difference method, *Chinese J. Geophys.*, 31,473-493.

Zhang, T.-R., S. Schwartz, and T. Lay, 1994, Multivariate analysis of waveguide effects on short-period regional wave propagation in Eurasia and its application in seismic discrimination, *J. Geophys. Res.*, 99, 21929-21945.